J. Fluid Mech. (1973), *vol.* 61, *part* 2, *pp.* 323–335
Printed in Great Britain

The effect of a bevelled trailing edge on vortex shedding and vibration

By M. E. GREENWAY AND C. J. WOOD
Department of Engineering Science, Oxford University

(Received 11 May 1973)

Experiments using a wind tunnel and a flow visualization technique in a towing tank were conducted to investigate the mechanism of vortex shedding from bevelled trailing edges. These reveal an important difference between the wake structures generated by heaving and steady motion. The suppression of vortex-excited vibration by means of bevelled trailing edges is attributed to the intermittency and rapid decay of the vortex trail resulting from an asymmetric circulation distribution in the vortex formation region.

1. Introduction

It is well known that many flow-induced vibrations of aerofoils, hydrofoils and other exposed structures are associated with the presence of a blunt trailing edge which sheds an alternating trail of vortices into the wake. This shedding is associated with periodic fluctuations in circulation about the body and the corresponding fluctuations in the lift distribution are responsible for the excitation of various modes of structural or other vibration.

Interest in flow-induced vibrations arises primarily of course because of the possibility of damage or catastrophic failure. However, an equally important reason in some cases is that undesirable noise levels are sometimes produced. This occurs, for example, in the case of hydrofoils or propeller blades which can 'sing' owing to high-frequency vibrations induced by vortex shedding.

Attempts to suppress such vibrations have often included detailed analyses of the vibrations themselves. In many cases, modes and frequencies have been predicted which are in good agreement with experimental data. Such methods can often be employed to make design modifications involving the mass, the stiffness or even the damping of the structure in order to suppress the natural response at those frequencies where fluid dynamic excitation is expected to occur.

An alternative, and potentially far more rewarding, approach to the problem is that which focuses attention upon the fluid dynamics of the excitation rather than upon the system response. This involves research into the fundamental mechanisms of vortex shedding and is clearly a long-term strategy.

This has not been the concern of design-oriented research, where, instead, the objective has been the solution of some immediate problems. This research has, however, led to a growth of empirical knowledge about trailing-edge shapes (Toebes & Eagleson 1961; Brepson & Leon 1972) which are very effective in

reducing vibration excitation. These shapes, which include base cavities, splitter plates and chamfered or bevelled trailing edges, are geometrically simple and can be applied as modifications to existing bodies in cases where vortex-induced vibrations are a source of difficulty. It is the object of the present paper to re-examine one of these shapes, the trailing-edge bevel, in an attempt to give a clearer understanding of the mechanism by which it achieves satisfactory suppression of vibrations.

The wake behind an asymmetrically inclined rear surface was first examined by Fage & Johansen (1927). However, their special case of an inclined flat plate differs from the general aerofoil or hydrofoil problem in that their separating shear layers were far from parallel to the undisturbed stream. For the present investigation, in order to achieve maximum simplicity and reasonable generality, it was decided to use models having rear surfaces which were parallel for some distance upstream of a sharp-cornered base. Very bluff shapes are thus excluded and it is ensured that not only are the separation points fixed and clearly defined, but also the initial width of the wake is defined, being approximately equal to the model thickness.

The other variable which is important in the wake formation mechanism is the state of the separating boundary layers and their size in relation to their spacing. This has been recognized, either explicitly or implicitly, by many investigators (e.g. Nash, Quincey & Callinan 1963; Gerrard 1966).

For models which are not too bluff, the boundary-layer condition at separation will be a function primarily of the Reynolds number based upon the chord or streamwise length of the model. This Reynolds number, therefore, and the thickness/chord ratio of the model may be regarded as jointly affecting the significant flow parameter, which is the relationship between the size and spacing of the separating shear layers.

Because of this joint influence it may be argued that, where no particular Reynolds number is specified for an experiment, there is no point in specifying a particular thickness/chord ratio either, provided always that the models are not too bluff. This reasoning provides the controlling philosophy behind the present experiments. It permits some flexibility in the design of models for different aspects of the study and also allows the qualitative conclusions about the flow mechanism to be applied tentatively over a fairly wide range of bodies on which the same vibration damping effects are observed.

2. Preliminary wind-tunnel tests

To check the efficacy of various trailing-edge bevel angles in suppressing vibration it was decided to conduct a preliminary series of experiments using a vortex-excited vibration system which could be reproduced easily and quickly under laboratory conditions. The system chosen was the acoustic vibration of the air volume surrounding an aerofoil model in a wind tunnel. This type of vibration was analysed by Parker (1967) and Franklin (1972). The physical system used here has been described previously by one of the present authors (Wood 1971). To construct it, a rigid two-dimensional wooden aerofoil was fixed

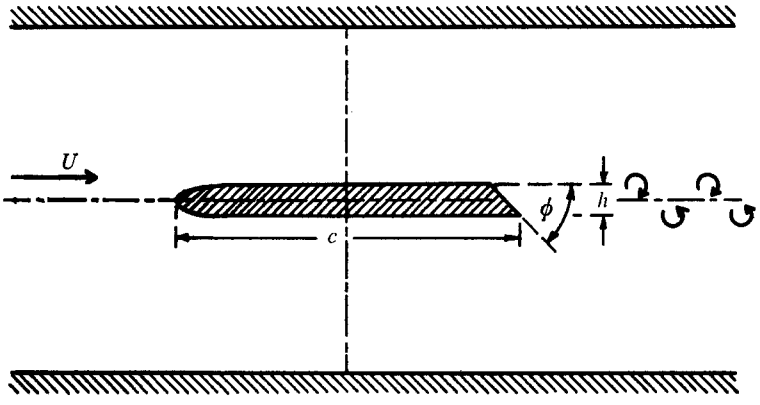

FIGURE 1. Diagram of model and resonant cavity.

centrally in the 460 × 320 mm working section of a small wind tunnel. Mounted between the rigid walls, the model spanned the shorter dimension of the working section and divided it into two equal passages. The optimum acoustic length for these twin passages was created by making the chord of the aerofoil equal to the larger transverse dimension of the tunnel (460 mm), thus forming the cavity shown in figure 1. The natural frequency of the cavity was 250–260 Hz and the pressure and velocity nodes are shown as horizontal and vertical lines in figure 1. Clearly this vibration is qualitatively analogous in several respects to the motion of a steady fluid stream about an aerofoil in transverse heaving vibration.

The model thickness for a considerable distance upstream of the truncated trailing edge was 38 mm. Using the Strouhal number 0·24 from Wood (1971) it was estimated that the vortex shedding frequency would reach 255 Hz at a tunnel speed of 40 m/s. This was a convenient point in the operating range and sufficiently high to provide adequate power for the resonance. The chord Reynolds number at this speed was $1{\cdot}3 \times 10^6$.

Resonant vibrations of this system gave rise to a clearly audible sound. In order to make amplitude comparisons, a Brüel & Kjaer condenser microphone was mounted on the tunnel floor near one of the pressure antinodes. The r.m.s. output signal was recorded in arbitrary units as the vibration was taken through resonance by slowly increasing the air velocity.

After a reference amplitude distribution had been recorded with the plain truncated trailing edge ($\phi = 90°$) the wooden model was modified successively to give trailing-edge angles ϕ of 75°, 60°, 45°, 30° and 20°. The consequent reduction in the amplitude of the resonance is shown in figures 2 and 3.

It can be seen from these results that there is no sudden elimination of vibration at any particular trailing-edge angle. Instead, there is a somewhat irregular, but apparently progressive reduction of intensity until, for trailing-edge angles below 30°, there is no evidence of any significant resonance remaining.

The vibration amplitude curves in figure 2 all begin to rise at roughly the

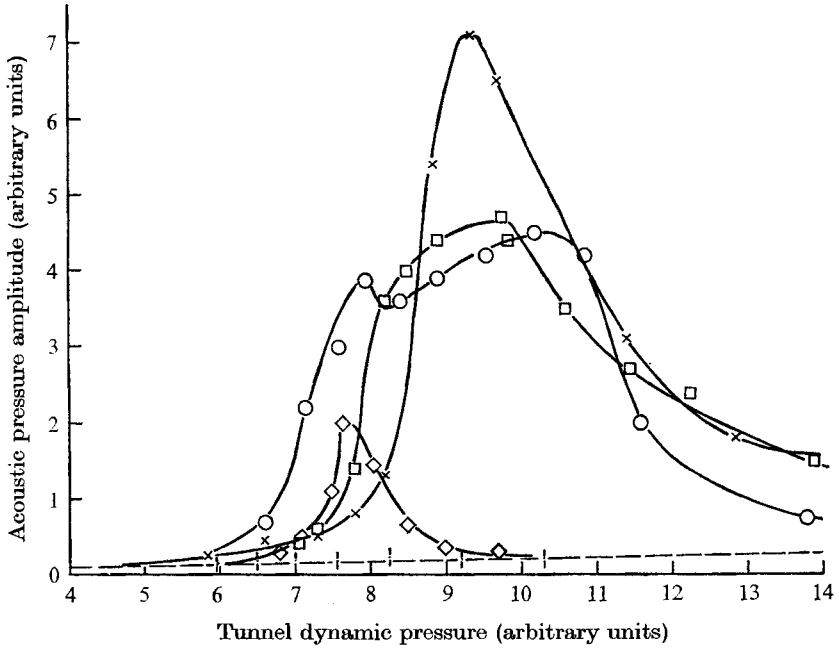

FIGURE 2. Variation of acoustic pressure amplitude with tunnel dynamic pressure for different trailing-edge angles ϕ. ———, tunnel empty; ×, $\phi = 90°$; ○, $\phi = 75°$; □, $\phi = 60°$, ◇, $\phi = 45°$; ¦, $\phi = 30°$.

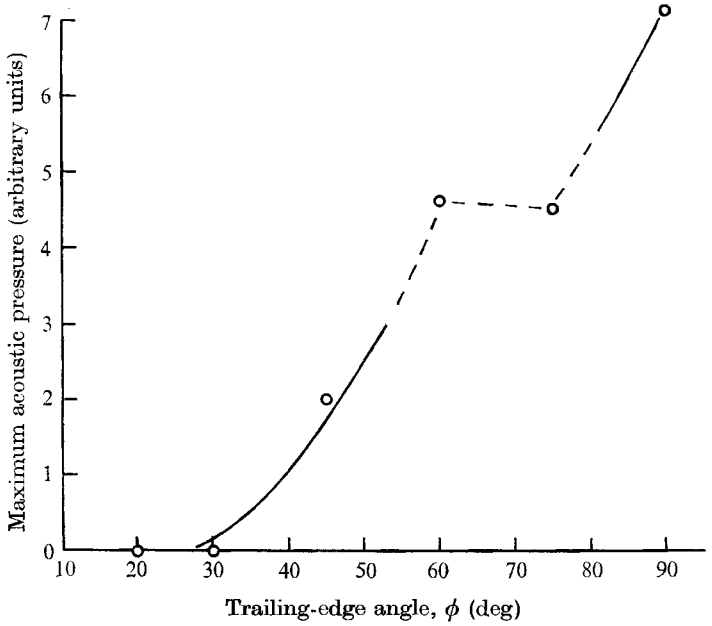

FIGURE 3. Decay of resonance peak with trailing-edge angle.

same wind velocity. This is somewhat below the nominal resonance speed and has been shown (Wood 1971) to be the lower limit of the frequency-locked range in which the shedding frequency is forced to coincide with the vibration frequency.

This observation, that the onset of vibration occurs under the same conditions for all trailing-edge angles, is significant because it suggests that the strength of the excitation, i.e. of the vortex shedding, in the quiescent state may not vary greatly with angle. This conclusion is supported by the flow visualization tests reported below.

Again comparing the vibration amplitude curves (figure 2) it is seen that the 90° curve continues to rise to a high peak at a tunnel speed well above the nominal resonance velocity before falling sharply as the frequency-locking limit is reached and the shedding frequency reverts to a value corresponding to the natural Strouhal number (Wood 1971). By contrast, the 45° curve shows that this shape does not exhibit the same capacity to correlate the shedding and lock the frequency. The amplitude rise is terminated therefore at a much lower speed and the peak value is reduced. The fact that this peak is actually below the nominal resonance velocity may also indicate a slight modification to the natural Strouhal number.

The decay in peak amplitude shown in figure 3 would have been relatively smooth, but for the puzzling absence of any marked difference between the peak amplitudes at base angles of 75° and 60°. This feature may be associated with the fact that the resonance curves in figure 2 do not exhibit the normal characteristics of the resonance mechanism but have broad and indefinite maxima. At present, the authors are unable to offer a satisfactory explanation for this observation. In recognition of the uncertainty about the mechanism at this point, the curve in figure 3 is drawn as a broken line.

During these measurements the microphone output meter was fairly heavily damped and therefore the curves in figure 2 represent amplitudes which were averages over times of order 1 s. From the audible sound, however, there was some indication that the reduction in average amplitude was accompanied by an increasing intermittency. This suggests the possibility that the vibration suppression achieved by bevelled trailing edges may not be due simply to a reduction of vortex shedding strength but may be caused by an intermittent interruption of the excitation. This possibility was examined further in subsequent experiments.

3. Flow visualization

The main part of the investigation consisted of a careful semiquantitative visualization of the wake flow from a series of bevelled trailing edges. The reason for this emphasis on flow visualization was the expectation that the known reduction in vibration excitation would be accompanied by observable variations in the strength and structure of the wake vortex trail.

Because previous experience (Wood 1971) with another trailing-edge shape had shown an important effect which only occurred in the presence of a vibra-

tion, it was not considered sufficient merely to study the wake under conditions of steady motion. Therefore the flow visualization experiments were conducted with the model moving both steadily and also with a superimposed transverse heaving oscillation.

3.1. *Equipment*

The study was performed using a two-dimensional model of thickness 41 mm and chord 165 mm. A common elliptical nose section having a semi-major axis of 82 mm was used to support a series of six parallel-sided rear sections. These were made quickly detachable by means of a sliding dovetail joint and had trailing-edge angles ϕ of 90°, 75°, 60°, 45°, 30° and 20°. The model parts were machined from Araldite blocks which were cast for lightness round expanded polystyrene core pieces.

The models were mounted under a trolley which moved on rails over a water tank 4·5 m long and 0·61 m wide. To produce a two-dimensional flow, each model was mounted vertically and extended through the water surface to reach within 2–3 mm above the tank floor, 380 mm below the surface.

The reason for moving the model rather than the water was to gain a convenient frame of reference for viewing the wake vortex shedding. A camera, mounted vertically below the glass floor of the tank, was focused upon a horizontal plane midway between the tank bed and the surface. The water in this plane was illuminated by 10 mm thick, parallel focused and collimated sheets of high intensity light emitted by two pairs of 1000 W, ultra high pressure, compact, mercury vapour lamps (G.E., BH6). Cooling was by compressed air jets, and dangerous emissions of mercury vapour were prevented by positive extraction and filtering of the cooling air from the sealed lamp housings. To prevent shadows, the two lamp units were mounted on opposite sides of the tank.

After the water had remained undisturbed for at least an hour, a suspension of neutrally buoyant (specific gravity 1·05) polystyrene beads 0·2 mm in diameter was introduced at the surface of the tank with minimum disturbance. The particles sank slowly into the light beam, where, shining brightly, they served as flow markers as the model traversed the tank. The motion of the particles in the horizontal plane was recorded photographically by a single exposure of approximately 100 ms duration. This yielded bright streaks on the film, where the 100 Hz flashing of the mercury vapour lamps served as a convenient and accurate time scale for velocity measurements.

Some of the longer particle streaks in figures 4–7 (plates 1–4) show the dots produced by the 100 Hz flashing. In the shorter streaks the dots merge together. To measure local velocities it is a simple matter to measure the distance from the beginning of the first dot to the beginning of the nth dot in a streak containing n dots and to record the time interval as $(n-1)/100$ s. The number n is of course common to all the streaks in any one photograph, so that even the short streaks can be measured in this way by regarding the nth dot as an inscribed circle at the end of the particle streak.

Absolute accuracy is limited by the film grain size, so that percentage errors are of course greater for the shorter streaks. However, the type of error is

random and the effective accuracy is greatly improved by averaging large numbers of measurements.

The choice of traverse speed in these tests was not based upon any criterion of dynamic similarity, but upon the capabilities of the photographic and associated measuring equipment. Thus a steady forward speed of 93·2 mm/s was used throughout. This motion was produced by a pulley and cable towing mechanism driven via a worm and pinion gearbox by a small induction motor. Traverse speed fluctuations were within 1 %. An added advantage of the low speed was that surface waves were less than 1 mm high and did not disturb the two-dimensional nature of the flow. The Reynolds number was $1{\cdot}4 \times 10^4$ based on the model chord and the boundary layers remained visibly laminar up to and beyond the separation points.

By making an approximate comparison of flat-plate boundary layers at the appropriate chord Reynolds numbers it may be estimated that, despite the much shorter model, the thickness of this boundary layer in relation to the model thickness is 2 or 3 times greater than that of the probably turbulent boundary layer in the preliminary wind-tunnel tests ($Re_c = 1{\cdot}3 \times 10^6$). This may partly explain the difference between the Strouhal number quoted below and that found in the wind tunnel. The coherence of the vortex shedding may also be affected, particularly in the steady state. However this difference is almost certainly obscured by the strong correlating effect of the vibration.

In addition to the steady forward motion of the trolley, a sinusoidal transverse oscillation of the model was also possible. This was achieved by means of a variable amplitude scotch yoke mechanism driving a secondary mounting plate on transverse linear bearings under the trolley. When mounted on this secondary plate the model could be oscillated relative to the trolley at frequencies up to 2 Hz. Despite the inertia of the moving parts and the forces exerted by the water, the crank speed could be maintained within $\pm 0{\cdot}35$ % throughout any oscillation cycle, thus providing a truly sinusoidal motion. This control was achieved by driving a d.c. motor from a specially designed servo-control unit.

3.2. *Test parameters*

Shedding-frequency measurements by stopwatch on the plain truncated model ($\phi = 90°$) in steady motion at 93·2 mm/s gave a mean value of 0·65 Hz. This corresponds to a Strouhal number fh/U of 0·286 based upon the model thickness h. As the trailing-edge angle was reduced, however, frequency measurements became increasingly difficult. The reason was that the shedding became more and more intermittent. A sequence of five or six vortices could often be seen in an apparently normal array, but these periods of regular shedding were increasingly interspersed with intervals of uncorrelated flow in which no distinct vortices were seen. (It should perhaps be noted at this point that the photographs in figures 6 and 7 were selected to illustrate the regular shedding pattern.) Unfortunately, the intervals of regular shedding were not sufficiently long for reliable frequency measurements to be made. Nevertheless, as there were no visual indications of any marked change, it was considered appropriate to

regard the frequency quoted above for the 90° model as the standard frequency for the whole series of tests.

The oscillation frequency for the unsteady tests was made equal to the standard shedding frequency in order to reproduce flow conditions corresponding to a resonant vibration. The amplitude, on the other hand, could not be set at any realistic value. Instead the scotch yoke was set arbitrarily at a crank radius y_0/h of 5 mm to give a dimensionless heaving amplitude $y_0/h = 0{\cdot}123$. This was large of course compared with many typical vibrations. However it should be emphasized that the object of the present tests was not to model a realistic vibration but rather to examine the response of the wake flow to an arbitrary motion of the body.

3.3. *Photographic method*

For detailed examination and measurement purposes a series of large scale photographs was taken on half-plate sized (120 × 165 mm) sheet film. Additionally a series of multiple picture sequences on 35 mm film was taken using an electrically driven automatic camera. This could be operated at up to 3 frames per second.

In order to make detailed comparisons possible between the wake flows for different trailing-edge angles, it was arranged that each photograph should be taken at exactly the same point in the oscillation cycle. This was achieved by means of a digital camera control unit.

In its basic form, the control unit was designed to receive and count electrical pulses from a simple photoelectric shaft encoder on the crank shaft of the mechanical oscillator. It could be set to trigger the camera at a predetermined pulse count following a starting pulse at zero crank angle. As the encoder pulses occurred at 0·1° intervals, the camera control unit was capable of controlling the camera with a corresponding accuracy. Time-lag errors in the shutter mechanism were eliminated by allowing the pulse count to continue until a final signal was received via the camera flash contacts indicating that the shutter was fully open. The total count then defined the crank angle, which was recorded for each photograph.

The same camera control system was used for the steady-motion cases, simply by setting $y_0/h = 0$ on the scotch yoke. However, it is clear that in these cases the vortex shedding could not be related in phase to the crank angle and the exposure points remained unavoidably random with respect to the vortex shedding cycle.

4. Results and discussion

4.1. *Qualitative observations*

Figures 4–7 (plates 1–4) show examples of the flows observed. They relate to four of the six trailing-edge angles, each taken both in (*a*) steady and in (*b*) oscillating motion. The unsteady cases were all photographed as the model reached zero displacement and maximum transverse velocity towards the obtuse side.

One of the effects noticed during the preliminary wind-tunnel tests was that the vortex-excited resonance appeared to decay not only through a reduction in amplitude but also by becoming more intermittent as the trailing-edge angle was reduced. Evidence of intermittency in the vortex shedding was also present in the wake photographs. By superimposing two or more photographs taken of the same model at the same phase angle it was possible to see that in the regular well-correlated shedding at $\phi = 90°$ the vortex patterns matched closely. This indicated a regular shedding cycle in which every part of the pattern was repeated. A similar comparison for any other angle, however, showed that the vortex positions did not correspond from one cycle to another, thus indicating that the shedding was not regular. This observation applies both to the steady cases and to those with oscillating motion.

It may also be noticed that figure 4(*b*) (plate 2) shows no sign of any three-dimensional variation, as evidenced by streakline intersections or other irregularities, whereas the vortices in other photographs are less clearly defined and three-dimensional distortions may have contributed to the observed decay. This is in general agreement with the observations of Koopman (1967).

The effect of the intermittency was to introduce a random character into the photographs at the smaller base angles. Some showed regular arrays of vortices while others showed only an uncorrelated turbulent wake. Figure 6(*a*) (plate 3) illustrates this feature well in that it shows the beginning of a regular pattern of vortices following immediately after a totally non-periodic section of the wake. In general, however, the photographs selected for display are those which were taken by chance, during the vortex shedding periods.

4.2. *Vortex strength measurements*

Having observed that the decay in excitation is at least partly due to a growing intermittency in the vortex shedding, it is of interest to determine whether or not there is also a decay in the strength of the shedding as indicated by the circulation about individual vortices. To measure the circulation about a vortex, a specially adapted two-component travelling microscope was used (Wood 1968). This had a turntable fitted in place of the normal object platform. After placing the centre of a vortex over the turntable axis it was possible to select a fixed radius in one co-ordinate direction on the two-component microscope and to measure tangential components of the particle streak lengths in the perpendicular direction. By selecting 30–50 particle streaks at known angular positions on the chosen radius it was possible, given the necessary scale factors, to perform a simple trapezium-rule integration to obtain an estimate of the dimensionless circulation Γ/Uh. The process was tedious, but it was automated by using a data recording system based upon a digital voltmeter coupled to potentiometers on the turntable pivot and on the microscope lead screws.

The results of these vortex strength measurements are plotted first of all as spatial variations in figure 8(*a*). Some care is required in the interpretation of these results, especially in cases where measurements from several photographs are superimposed (e.g. $\phi = 75°$ or $\phi = 60°$). Because the shedding is intermit-

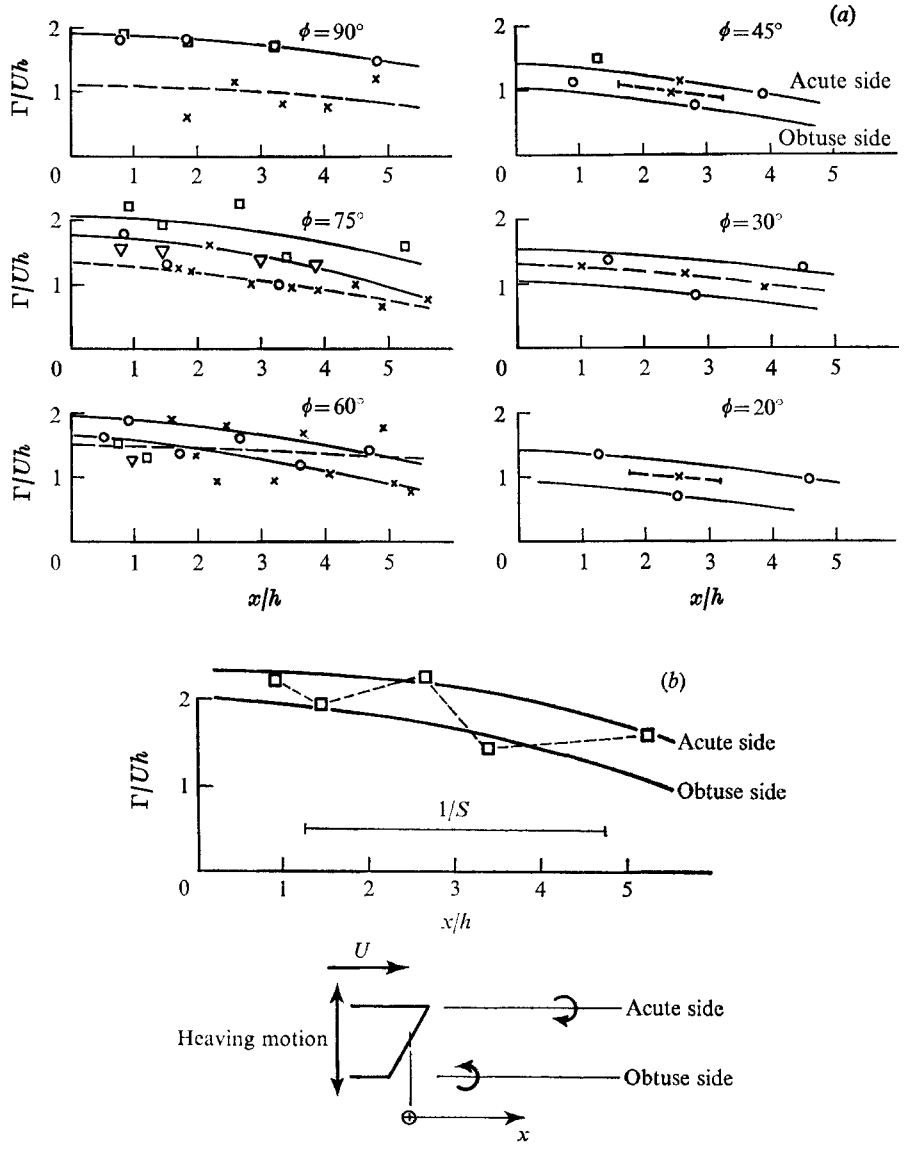

FIGURE 8. (*a*) Variation of vortex strength with streamwise position. ○, ▽, □, oscillating (symbols distinguish between photographs); — × —, steady. (*b*) Key to interpretation of (*a*).

tent in the presence of bevel, there are distinct variations between photographs and the impression given is of a confused scatter in the points. However, when each photograph is considered in isolation a more consistent pattern emerges. Points from different photographs are distinguished therefore in figure 8(*a*) by the use of distinctive symbols. Also the pattern is illustrated in figure 8(*b*), which shows the results of a single oscillating test, extracted from the $\phi = 75°$ graph in figure 8(*a*).

The most obvious feature of this pattern is of course the expected decay of the vortices with increasing age (or increasing distance from the trailing edge).

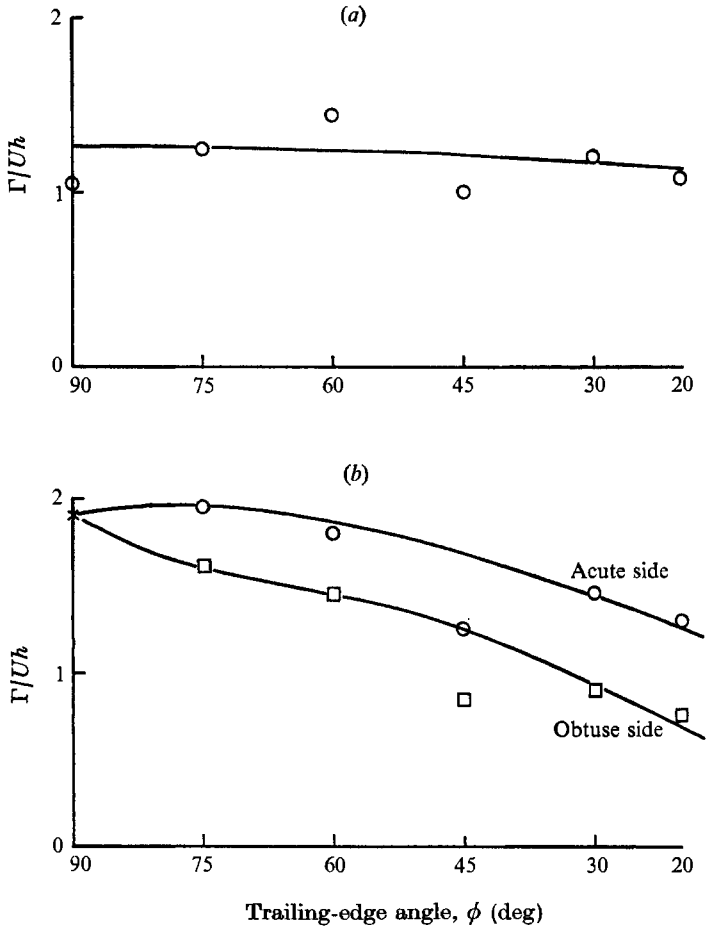

FIGURE 9. Variation of vortex strength with trailing-edge angle ϕ.
(*a*) Steady. (*b*) Heaving.

This trend is recognized in all the curves in figure 8(*a*) and it is to eliminate this decay that figure 9 was drawn, by cross-plotting from figure 8(*a*) at a fixed but arbitrary streamwise position ($x/h = 2$).

A second and most important feature is that the vortices shed from the acute corner are stronger than those from the obtuse corner. It is to show this asymmetry that two solid curves have been drawn for each base angle in figure 8(*a*). Naturally the difference vanishes when the model is symmetrical ($\phi = 90°$) but the striking fact is that the phenomenon is associated exclusively with oscillating models. When the motion is steady the measured vortex strengths, although displaying the usual scatter, show no discernible tendency to be consistently stronger on one side of the wake than on the other. This conclusion is not proved in figure 8(*a*) as drawn because distinguishing between vortex rows and between photographs would cause confusion. It was reached however only after identifying each measured vortex and comparing it with others on the same photograph, taking account of the streamwise decay. On the strength of this conclu-

sion, the average vortex strength for the steady cases is drawn as a single broken line.

The third observation is that the trailing-edge bevel inhibits the increase in vortex shedding strength which is normally associated with oscillating bluff bodies. Figures 8(*a*) and 9 confirm that a plain truncated base sheds a stronger and better correlated vortex trail when oscillating than it does in steady motion. The vortices also form closer to the model (figures 4(*b*), 4(*a*), plate 1). With decreasing base angle, although the vortices continue to form close to the oscillating model, this difference in shedding strength is progressively reduced until at $\phi = 30°$ and $\phi = 20°$ the few vortices which do appear have the same average strength as those shed in steady motion.

It would obviously be instructive to correlate these observations with actual measurements of the fluctuating forces on the model. Unfortunately the equipment for making these measurements is not yet complete, so that the present discussion is limited to a qualitative assessment only. Nevertheless, it is possible to make two significant deductions.

The first applies to steady motion. Since the trailing-edge bevel produces no measurable reduction in the strength of the vortex shedding, but only growing intermittency, it may be argued that any reduction in vibration excitation in the quiescent state arises because of irregularity in the periodic lift force rather than from a significant reduction in amplitude.

In the presence of an actual vibration, however, the effect is rather different. Here the effect of the bevel is to reduce not only the coherence but also the amplitude of the shedding. This is clearly an important aspect of the vibration damping mechanism in that it contributes to the decay of the vortex trail specifically under conditions of model vibration. Without such a reduction, as the 90° results show, a vibration can amplify the vortex shedding and thereby actually increase the excitation which caused it in the first place. The importance of this dynamic damping effect as opposed to the simple inhibition of vortex shedding in the quiescent state was demonstrated in a previous experiment by one of the present authors (Wood 1971). That experiment showed that the vibration damping which is achieved by a simple trailing-edge cavity occurs despite the fact that the cavity has no effect whatsoever on the quiescent vortex shedding. The mechanism in that case could be seen clearly in flow photographs and was associated entirely with the motion of the model.

5. Conclusions

The present visual investigation of the effect of a bevelled trailing edge has drawn attention to several important features of the flow in the near wake.

First, in the absence of vibrational motion of the body, a bevelled trailing edge has very little effect upon the strength of the vortex shedding. However, it does appear to destabilize the wake vortex trail and lead to intermittency and a consequent reduction in the excitation.

When a blunt-based aerofoil vibrates in a heaving motion the vortex trail behind the truncated trailing edge forms closer to the body and is stronger and

better correlated. This provides an increased excitation which is caused by the vibration itself. Under these dynamic conditions the effect of a trailing-edge bevel is to destroy this amplification effect. Not only is the mean vortex strength reduced to the quiescent level but also an asymmetry is introduced in which the vortices from the acute corner become stronger than those from the obtuse corner. This suggests that there is a change in the circulation distribution mechanism in the vortex formation region and its effect is to cause a serious instability in the vortex trail which vanishes within one or two cycles.

These effects of decreasing the trailing-edge angle are progressive. Satisfactory damping appears to be achieved for angles of 30° or less.

The work described in this report was supported by a Ministry of Defence research grant (Ref. N/CP 10864/72/DC28(1)/R176). Much of the equipment used was designed and developed with the aid of a Science Research Council grant (Ref. B/SR 9584). The majority of this development work was carried out in 1970–71 by Mr M. E. Byford, to whom the authors wish to express their appreciation.

REFERENCES

Brepson, R. & Leon, P. 1972 Vibrations induced by von Kármán vortex trail in guide vane bends. *I.U.T.A.M.–I.A.H.R. Symp. on Flow-Induced Structural Vibrations, Karlsruhe.*

Fage, A. & Johansen, F. C. 1927 The structure of vortex sheets. *Aero. Res. Counc. R. & M.* no. 1143.

Franklin, R. E. 1972 Acoustic resonance in cascades. *J. Sound Vib.* **25**, 587.

Gerrard, J. H. 1966 The mechanics of the formation region of vortices behind bluff bodies. *J. Fluid Mech.* **25**, 401.

Koopman, G. H. 1967 The vortex wakes of vibrating cylinders at low Reynolds numbers. *J. Fluid Mech.* **28**, 501–512.

Nash, J. F., Quincey, V. G. & Callinan, J. 1963 Experiments on two-dimensional base flow at subsonic and supersonic speeds. *Nat. Phys. Lab. Aero. Rep.* no. 1070.

Parker, R. 1967 Resonance effects in wake shedding from parallel plates: calculation of resonant frequencies. *J. Sound Vib.* **5**, 330.

Toebes, G. H. & Eagleson, P. S. 1961 Hydroelastic vibrations of flat plates related to trailing edge geometry. *Trans. A.S.M.E.* D **83**, 671.

Wood, C. J. 1966 Visualization of an incompressible wake with base bleed. *J. Fluid Mech.* **29**, 259.

Wood, C. J. 1968 A travelling microscope with semi-automatic digital output. *J. Sci. Instrum.* **1** (2), 475.

Wood, C. J. 1971 The effect of lateral vibrations on vortex shedding from blunt-based aerofoils. *J. Sound Vib.* **14**, 91.

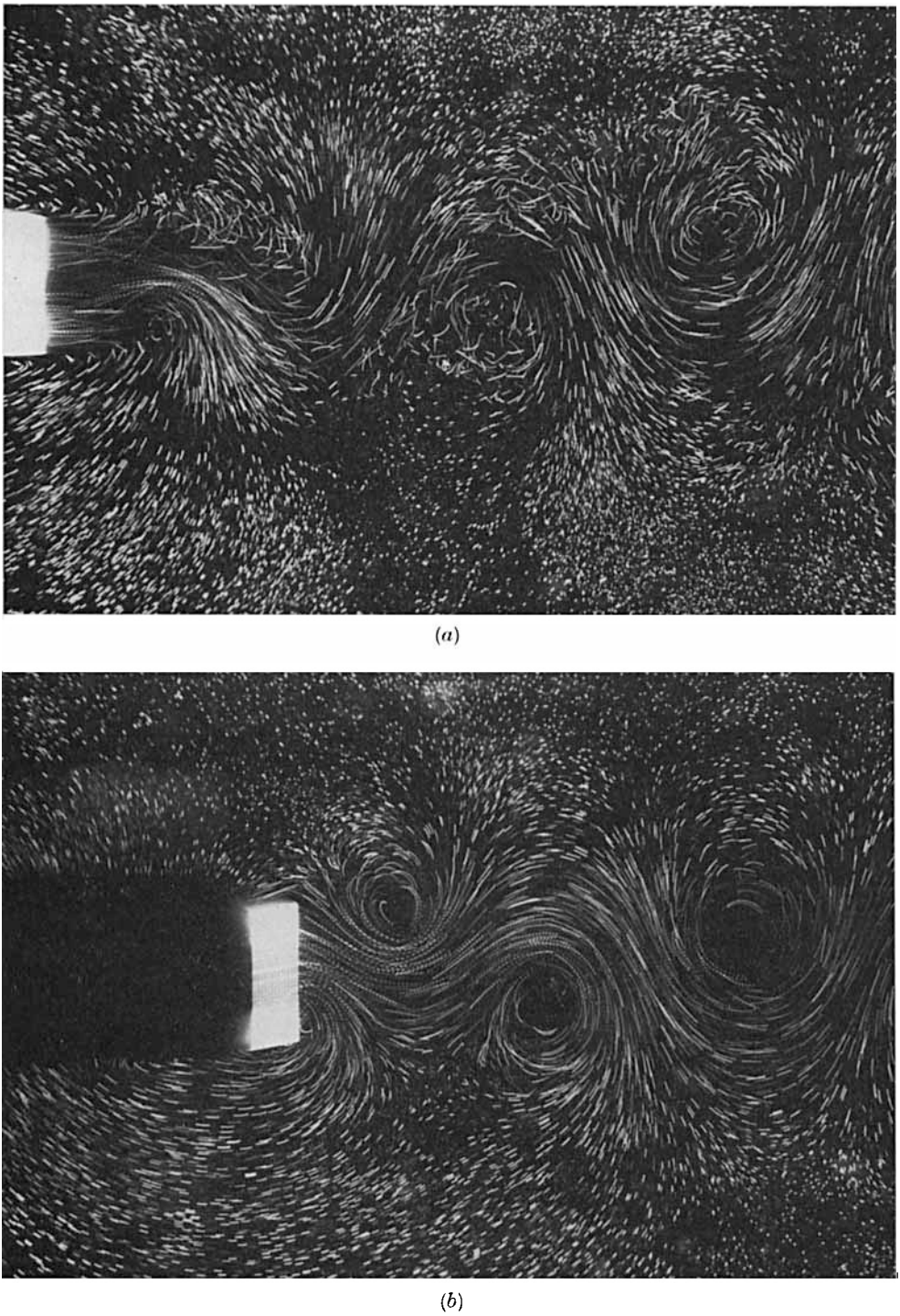

(*a*)

(*b*)

FIGURE 4. Wake in (*a*) steady and (*b*) heaving motion. $\phi = 90°$.

(*a*)

(*b*)

FIGURE 5. Wake in (*a*) steady and (*b*) heaving motion. $\phi = 75°$.

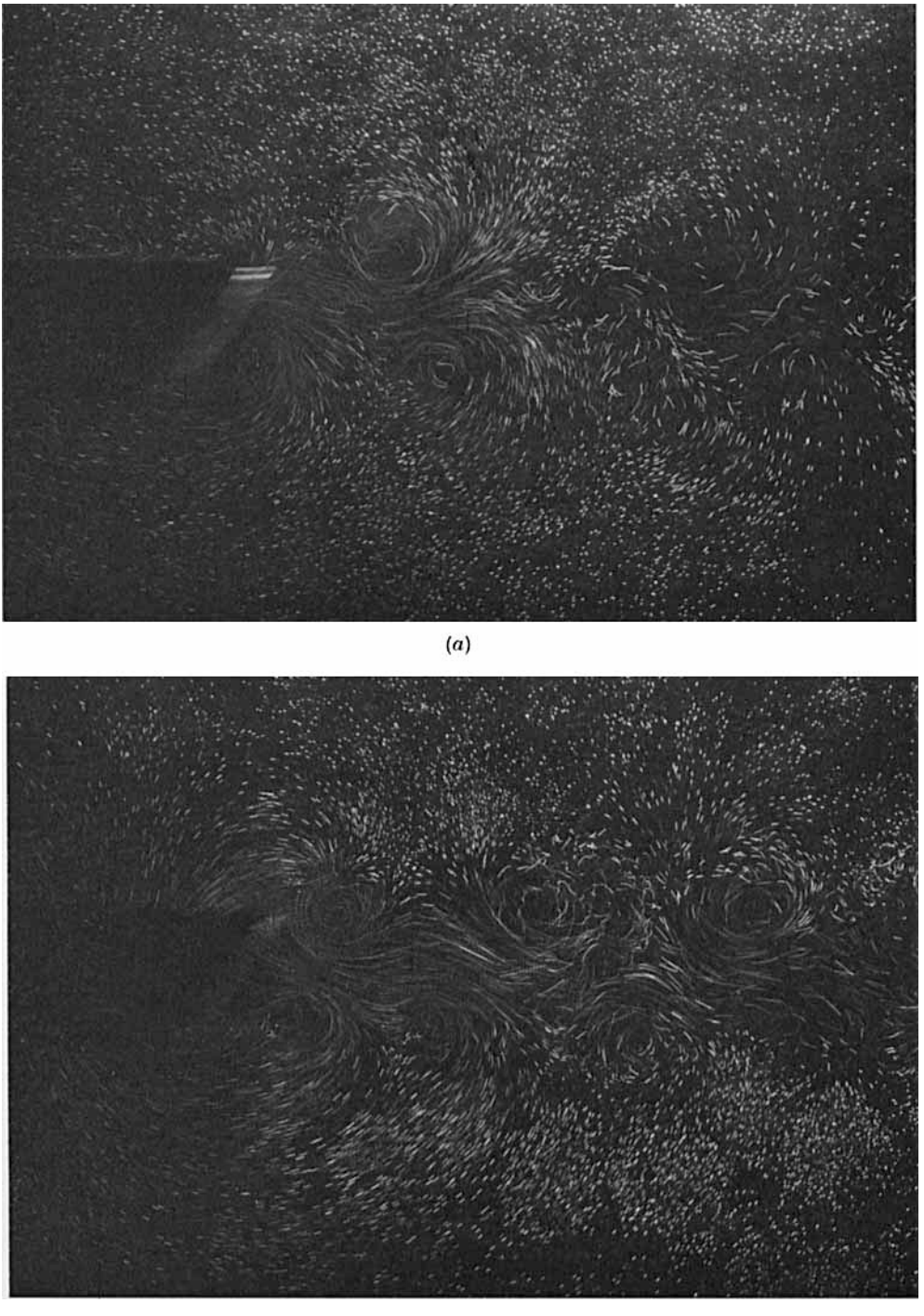

(*a*)

(*b*)

FIGURE 6. Wake in (*a*) steady and (*b*) heaving motion. $\phi = 60°$.

(*a*)

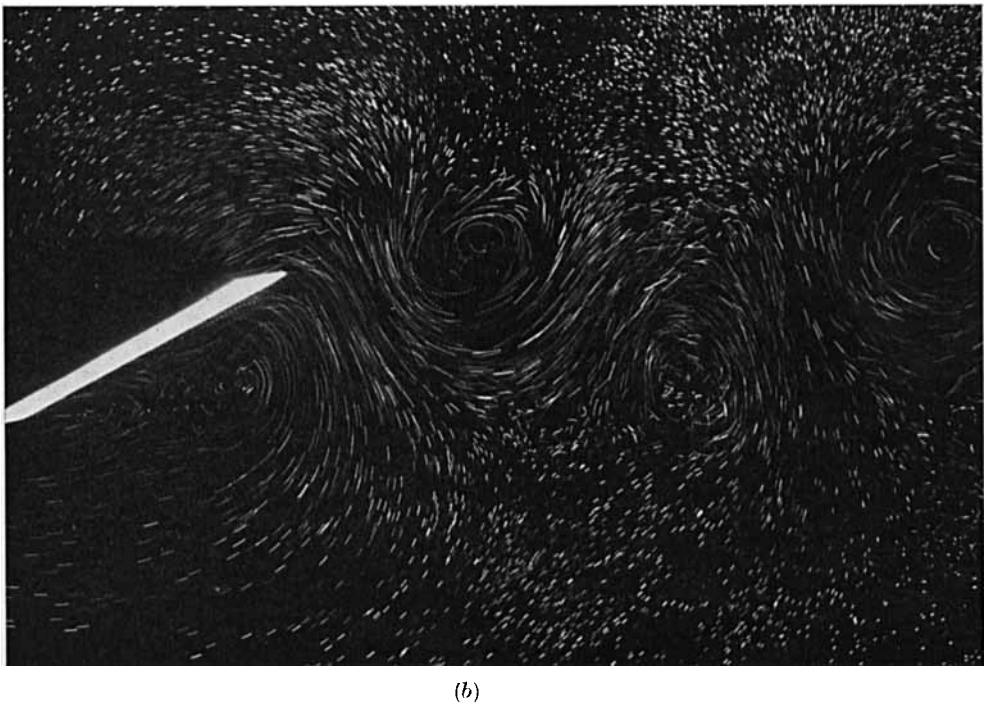

(*b*)

FIGURE 7. Wake in (*a*) steady and (*b*) heaving motion. $\phi = 30°$.